DAΦNE TECHNICAL NOTE

INFN - LNF, Accelerator Division

Frascati, December 12, 1997

Note: **RF-20**

OPTIMISED DESIGN OF A CRAB CAVITY EXAMPLE FOR DAΦNE

*P. Arcioni *, M. Migliorati #, L. Palumbo #, B. Spataro @*

(∗) Dipartimento di Elettronica di Pavia, Via Ferrata 1, 27100 Pavia, Italy
(#) Università di Roma " La Sapienza", P.le Aldo Moro 2, I-00185 Roma, Italy
(@) INFN- Laboratori Nazionali di Frascati, C.P. 13, 00044 Frascati, Italy

1. Introduction

Recent projects of e^+ e^- high luminosity colliders (Factories) [1,2] foresee crossing angle in the interaction point (IP), small enough to avoid luminosity degradation and synchro-betatron resonance excitation. This choice is confirmed by simulation programs and measurements [3,4,5,6]. Nevertheless, since the Factories will operate at a never reached current intensity , the crab-crossing scheme, originally proposed by R. Palmer [7] to maximise the luminosity in multibunch linear colliders, still remains an option for Factory projects, as, for example, for the KEKB Factory, where a vertical crab crossing cavity is foreseen [8].

In the crab-crossing scheme an RF deflecting cavity is used to tilt the bunch in the transverse direction around its centre, thereby making it collide head-on with the opposite bunch at the IP. A second cavity symmetrical with respect to IP cancels the tilt after the interaction. The same effect can be obtained with the use of longitudinal accelerating RF cavities located at a non-zero dispersion region [9].

In this work we present the design strategy to improve the performance of a crab-cavity. Though the actual design has been optimised for DAΦNE Φ-Factory, the proposed criteria are of general application.

In the second section of this paper we review briefly the crab-crossing scheme. In the case of DAΦNE, the voltage required to deflect the beam is very low, about 100 KV, due to the relatively low particle energy [10]. The main drawback is the multibunch instability driven by the parasitic modes trapped in the cavity. The equations to evaluate longitudinal and transverse growth rates are presented in section 3. As already seen for the main RF cavity [11,12], for high current regime a bunch-by-bunch feedback system cannot control the instabilities due to HOMs. Therefore six dampers connecting the main body of the cavity to dissipative terminations have been foreseen. The fundamental mode must be damped separately by using a feedback system or by decoupling it from the beam harmonics by means of a special dedicated tuner. The RF cavity design, operating on the deflecting mode TM_{110}, is chosen from the comparison between two cell shapes, "rounded" and "nosecone". In section 4 a general criterion for the design of the cavity is illustrated. The remaining two sections are dedicated to the comparison between rounded and nosecone performance, by analysing the results of 2D and 3D simulation codes.

2. The Crab-Crossing Scheme

The crab-crossing scheme allows the beams to collide head on when the trajectories have a crossing angle θ in the IP. A crossing angle at the IP allows a reduced bunch spacing than the head on collision, increasing consequently the collision frequency and therefore producing luminosity enhancement. Furthermore, it has been shown that in storage ring colliders the crab-crossing does not excite synchro-betatron beam-beam resonances [10].

Figure 1 shows schematically its operating scheme. An RF cavity located at 90 degrees betatron phase advance from the IP, gives a first transverse angular kick $\theta/2$ to the head of the bunch and a kick of opposite sign to the tail. After $\pi/2$ phase advance, the bunch, tilted around its centre, collides head on with the opposite one. A symmetrical cavity with respect to the IP cancels the tilt after the interaction.

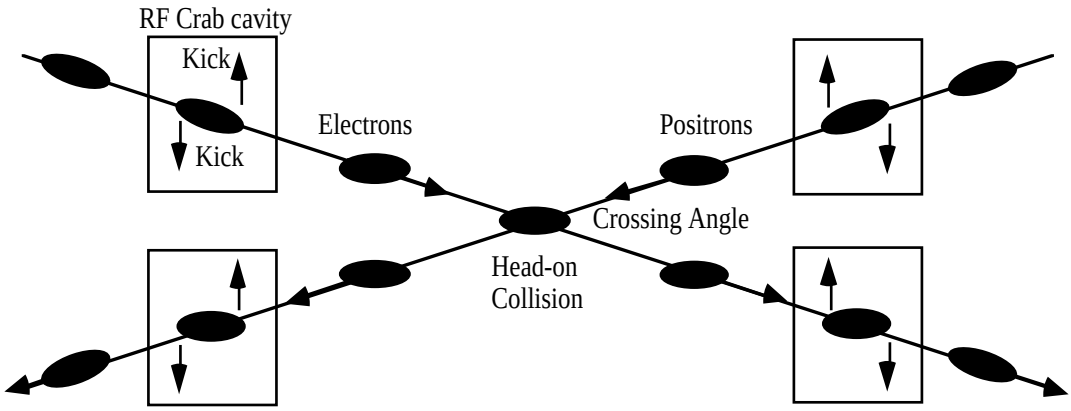

Figure 1: The crossing angle scheme.

If we assume a bunch length σ_z much smaller than the wavelength λ of the crab-crossing cavity, and a crossing angle θ small enough that $\tan(\theta) \approx \theta$, then the peak voltage required to tilt the bunch can be written as

$$\hat{V} = \frac{\theta\lambda\left(E_o/e\right)}{4\pi\sqrt{\beta^*\beta_c}} \tag{1}$$

where E_o is the nominal energy, β^* the beta-function at the IP, and β_c the beta-function at the RF crab cavity location. For DAΦNE the voltage is very low, about 100 KV, due to the relatively low particle energy, while for KEKB the required kick is about 1.4 MV [8].

3. Parasitic Modes

The DAΦNE collider has been designed with a maximum number of 120 bunches/beam. Electrons and positrons circulate in two separate rings; the total number of the particles in each ring is about 10^{13}. The choice to achieve the required luminosity with a large current makes the operation of the machine very critical with respect to coupled bunch instabilities. HOMs damping constitutes one of the main problems in high current accelerators. The beam spectrum may couple with HOM modes of the deflecting cavity, and if R/Q and Q are high enough, the beam can be strongly excited and even lost. The Q values of the parasitic modes must therefore be drastically decreased to avoid multibunch instabilities. Moreover, the deflecting mode used for the crabbing operation is not the lowest mode of the cavity. This requires a particular cure of the trapped parasitic modes, which must be treated with a global damping approach. A suitable damping scheme, already used for the accelerating cavity resonator of DAΦNE [11], consists of waveguides terminated by RF transitions to coaxial cables.

An estimate of the effectiveness of the damping scheme can be obtained by calculating the rise time of the multibunch instability due to the parasitic modes: for a good design this quantity should be large enough to allow a bunch-by-bunch feedback system to be effective [12]. The multibunch instability growth rates for Gaussian bunches can be written as [13]

longitudinal

$$\frac{1}{\tau_o} = \frac{I_b m \alpha_c}{\omega_s (E_o / e) 2\pi\sigma_\tau^2} I_m\left(p^2\omega_o^2\sigma_\tau^2\right)\frac{R_s}{p}\exp\left(-p^2\omega_o^2\sigma_\tau^2\right) \tag{2}$$

transverse

$$\frac{1}{\tau_o} = \frac{I_b \omega_r}{4\pi(E_o / e)Q} R_\perp^{URMEL} \\ I_m\left[\sigma_\tau^2\left((-p+Q)\omega_o - \omega_\xi\right)^2\right]\exp\left[-\sigma_\tau^2\left((-p+Q)\omega_o - \omega_\xi\right)^2\right] \tag{3}$$

with I_b the beam current, m the oscillation mode number, α_c the momentum compaction, ω_s the unperturbed synchrotron frequency, σ_τ the bunch length in time units, $I_m(x)$ the modified Bessel function, R_s the longitudinal shunt impedance, ω_o the angular revolution frequency, ω_r the HOM resonant frequency, Q the betatron number, $R_\perp^{URMEL}$ the transverse shunt impedance as given by the URMEL code [14], $\omega_\xi = Q\omega_o\xi / \alpha_c$, and ξ the chromaticity.

In the worst case of full coupling condition, if $m\omega_s \ll \omega_r$, the instability rise time obtained for both the longitudinal and transverse cases is

$$\tau = \frac{2\tau_f}{\sqrt{1 + 4\dfrac{\tau_f}{\tau_o}} - 1} \tag{4}$$

with τ_f the HOM filling time.

Equation (4) will be used to calculate the instability rise times as shown in the following sections.

4. Design Criteria of the RF Cavity

In order to deliver with good approximation a transverse momentum proportional to the particle distance from the centre of the bunch, and assuming a bunch length σ_z = 3 cm, the operating frequency was chosen to be 368 MHz.

Our goal for the optimisation of the cavity shape is not only to save RF power but also to minimise the HOMs content of the cavity itself.

The dependence of the relevant RF parameters of the pill-box cavity on the radius/gap ratio of the lowest monopole and dipole modes, is well known [14]. This behaviour is reproduced when the apertures for the beam are introduced, at least until the mode frequency remains below the beam aperture cut-off. This fact suggested the possibility of finding an optimum shape also for a deflecting cavity resonator. Indeed, extensive simulations using the URMEL code [15] showed that a similar behaviour is reproduced in cavities with regular shapes, like rounded or nosecone cavities. But it showed, also, that HOMs impedances were still too high to fulfill the design specifications. For this reason waveguide dampers were used, to decrease the Q-factors of the HOMs to such low values to reduce the strength of instabilities.

Moreover, the transverse shunt impedance of the unwanted polarisation of the deflecting TM_{110} mode is high. It must be strongly shifted in frequency by an azimuthally asymmetric profile and damped. In order to solve this problem, a polarised cavity shape derived from a 2D design was chosen. Therefore, two-dimensional codes are no more suited for the simulations. To have a quantitative estimate of the HOMs damping in the crab cavity, we carried out several computer simulations using the 3D-MORESCA code [16,17].

5. Rounded and Nosecone Cavities: 2D - Simulations

We started the study from the 2D design of two relevant examples, rounded and nosecone, working at 368 MHz and having a high transverse shunt impedance value [14].

In the nosecone cavity there are five trapped parasitic modes while only two in the rounded one. The trapped parasitic modes of the nosecone cavity are the fundamental TM_{010} mode, an unwanted polarisation of the TM_{110} dipole mode, the first TM_{011} monopole mode, two polarisations of TE_{111} dipole mode; those of the rounded cavity are the fundamental TM_{010} mode and the unwanted polarisation of the TM_{110} dipole mode. Our main concern is to damp all HOMs with waveguides having the cut-off frequency beyond the operation one. In order to push the frequencies of the trapped TM_{011} and TE_{111} modes of the nosecone cell beyond the waveguide cut-off frequency, a proper longitudinal profile has been provided. In this case, 20% of the transverse shunt impedance of the working mode is lost.

Figures 2 and 3 show the axisymmetric cavity shapes, rounded and nosecone.

To minimise the broadband impedance, tapers from the cell iris to the beam pipe radius of 4.5 cm have been included [18].

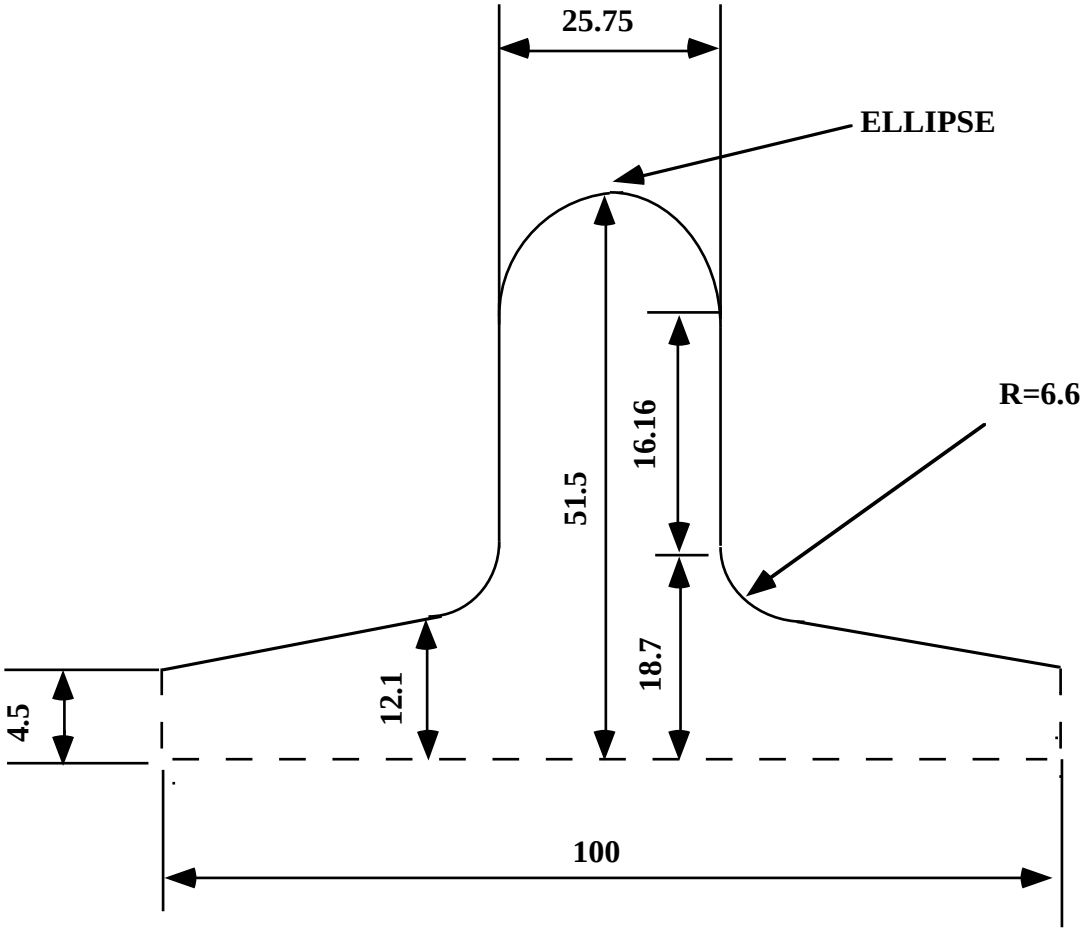

Figure 2: Axisymmetric rounded cavity shape. Dimensions in cm.

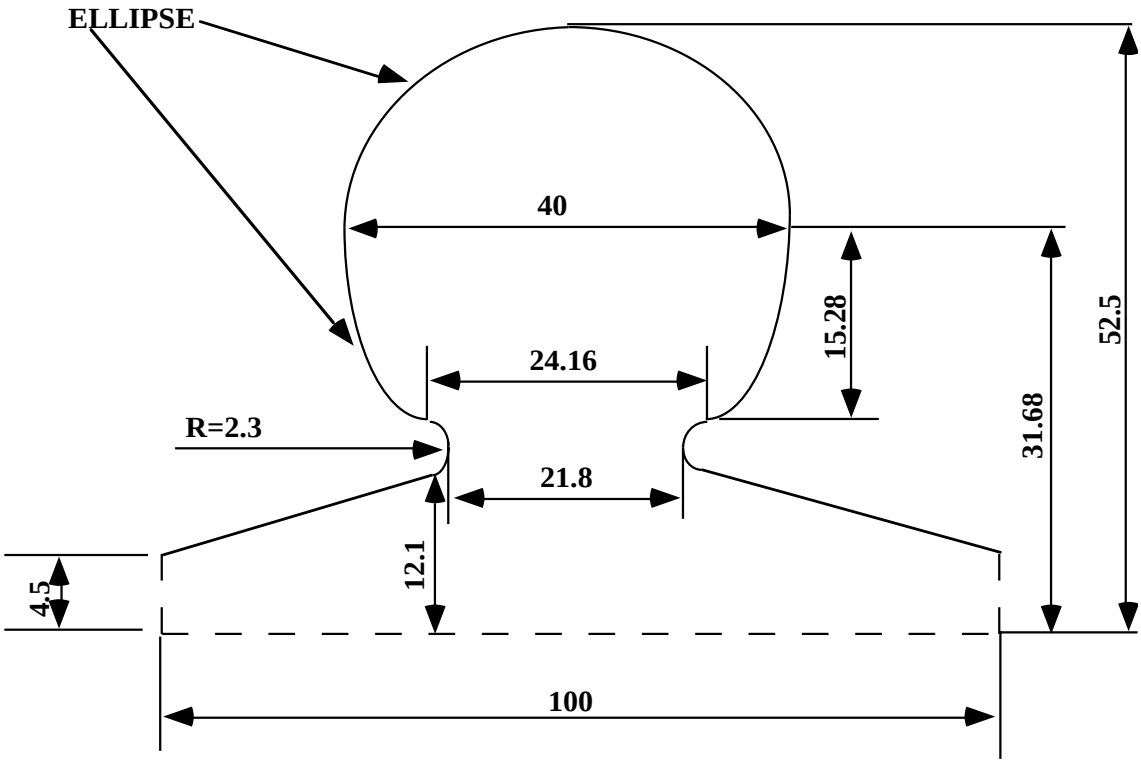

Figure 3: Axisymmetric nosecone cavity shape. Dimensions in cm.

In tables 1 and 2, the RF properties of the crabbing TM_{110} mode, the main RF parameters of the lowest frequency modes and the longitudinal and transverse loss factors of the two cavities are compared. The Kilpatrick criterion [19] for the two kinds of cells is fully fulfilled. Assuming 100 KV deflecting voltage, the power loss is kept very low, of the order of some KW. The nosecone cavity seems to perform better, as for the ratio between the loss factor of the dipole HOMs and the one of TM_{110} (equal to 1.76 and 2.61 for the nosecone and the rounded cavities respectively). The same holds true for the monopole modes (2.31 against 2.67). Only the ratio $E_{\max}/E_o$ is not very good.

Table 1

Crabbing Mode	*Nosecone*	*Rounded*
Frequency (MHz)	367.702	368.288
Geometry Factor Q^*R_s (Ω)	309	255
Transverse Shunt Impedance (MΩ) at 4.5 cm	2.94	1.66
Stored Energy (Joule)	0.045	0.066
Dissipated Power (KW)	1.70	3
Max. Sur. El. Field (MV/m) $E_{\max}$	1.77	1.21
Max. Sur. Mag. Field (Oe) $H_{\max}$	11.98	19.4
Average Electric Field (MV/m) E_o	0.245	0.245
$E_{\max}/E_o$	7.22	4.9
$H_{\max}/E_o$ (Oe m/MV)	48.9	79.2
Beam Power at 1 mm (KW)	1.16	1.16

Table 2

		Nosecone	*Rounded*
TM_{110} mode	Frequency (MHz)	367.702	368.288
	R'/Q (Ω)(at 4.5cm)	47.62	32.6
	Q	61724	51000
	Loss Factor (V/pC/m)	1.16	0.84
Dipole Modes	Loss Factor (V/pC/m)	2.04	2.19
TM_{010} mode	Frequency (MHz)	206.679	246.673
	R/Q (Ω)	96.21	66.48
	Q	45824	41300
	Loss Factor (V/pC)	0.055	0.051
Long. Modes	Loss Factor (V/pC)	0.127	0.136
TM_{011} mode	Frequency (MHz)	455.583	674.856
	R/Q (Ω)	2.3	5.84
	Q	44311	46800
TE_{111} mode	Frequency (MHz)	461.401	536.192
	R'/Q (Ω)(at 4.5cm)	0.25	4.96
	Q	50702	54900

The TM_{010} mode must be damped separately by using a feed-back system [20] or by decoupling it from the beam harmonics by means of a special dedicated tuner.

A suitable transverse asymmetric profile to separate in frequency the unwanted polarisation of the TM_{110} mode is required. The cells are of the same type and are derived from a 2D model like ours.

The HOMs can be extracted by wide-band global dampers. In order to study the behaviour of the two polarised cavities with waveguides absorbers, nosecone and rounded, 3D-simulations were needed, as it will be described in next section.

6. 3D - Simulations

The 3D simulations of the crab cavity have been performed to obtain two main design goals: i) to remove the degeneracy between the horizontal and vertical polarised deflecting (dipole) modes, and ii) to have a quantitative estimate of the longitudinal and transverse coupling impedances of the HOMs of the cavity connected to the waveguide absorbers. In the following the modification performed on the two geometries of figures 2 and 3 studied in the 2D simulations, i.e., nosecone and rounded cavity are considered, and the respective advantages and drawbacks are discussed.

In both cases, the degeneracy of the deflecting mode (quasi-TM_{110} mode) has been removed by deforming the cavity shape to change the revolution symmetry of the cavity into a reflection symmetry with respect to the two orthogonal planes α and β (horizontal and vertical planes, see figure 4a). In this way the resonant frequencies of the two quasi-TM_{110} modes are modified to different extents: thus it is feasible to suppress the unwanted polarisation by the waveguide dampers, which are designed in such a way to have their cut-off frequency between the two modified resonant frequencies. Note that in the modified cavity it is necessary to consider two different transverse coupling impedances ($Z_{\perp h}$ and $Z_{\perp v}$), according to the displacement of the beam in the horizontal or vertical plane [17].

The HOM dampers consist of six waveguides, connected to the cavity in two groups of three, placed along the periphery of the cavity, 120° apart one from each other (see figure 4b). This arrangement has the advantage of preserving the reflection symmetry of the cavity with respect to the plane γ, perpendicular to the beam axis, and, consequently, to produce a deflecting field, which is also symmetric with respect to that plane.

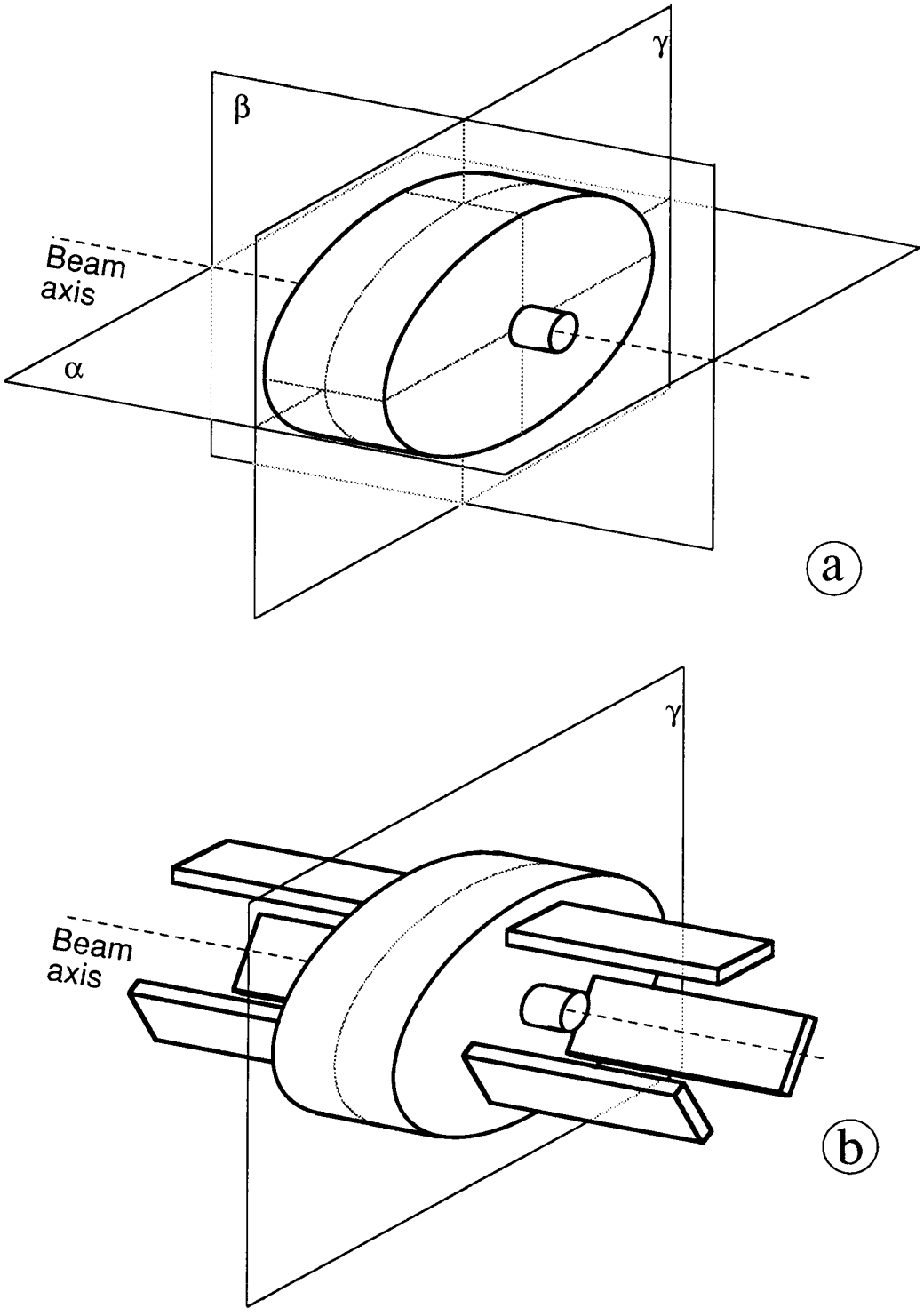

Figure 4: Sketch of a crab cavity: a) the symmetry planes of a simple pill box cavity, deformed to suppress the degeneracy of the deflecting modes;
b) the same cavity connected to the waveguide dampers.

6.1 Nosecone Cavity

In this case it is possible to remove the degeneracy of the deflecting mode by deforming the cavity in the nose region (removing the nose in correspondence of the vertical plane) or on the periphery (realizing an elliptical cross-section in correspondence of the γ plane, with the major axis on the horizontal plane). The two kinds of deformation act in the same way on the splitting of the resonant frequencies of the degenerate quasi-TM_{110} modes. In fact, both decrease the resonant frequency of the mode having vertical polarised magnetic field in the beam region, i.e., the mode that causes the horizontal tilt of the bunches, and increase the resonant frequency of the horizontally polarised mode. The effect on the transverse coupling impedances, however, is different. Some preliminary simulations have showed that the deformation on the periphery decreases the value of $Z_{\perp h}$ of the mode used for the crabbing action, and increases the value of $Z_{\perp v}$ of the mode that must be suppressed. On the contrary, the modification of the nose shape increases $Z_{\perp h}$ and decreases $Z_{\perp v}$. For this reason we chose to modify the geometry in the nose region, since, in this case, the transverse coupling impedance of the useful mode is higher and the damping of the unwanted mode is easier.

The design of the nosecone cavity starts with the definition of the nose geometry to obtain a splitting of the resonant modes of the quasi-TM_{110} modes of about 50 MHz, that is sufficient to suppress the unwanted mode with the waveguide dampers. A cavity without waveguide dampers is considered at this stage of the design. The numerical simulations showed that, to obtain this result, it is necessary to completely remove the nose at the vertical plane, deforming progressively the depth of the nose from full depth to zero depth in an angular sector of ±60° around the vertical plane (see figure 5). Table 3 shows the parameters of interest, i.e., the resonant frequencies, the Q-factors and the real part of the coupling impedances, for the first monopole and dipole modes calculated by MORESCA [18] and POPBCI [17] up to 500 MHz. For reference, in the case of the axisymmetric cavity, the same code delivered, for the first dipole mode (quasi-TM_{110} mode) a resonant frequency of 390 MHz, a Q-factor of 52500 and a value of 21.1 KΩ/mm for $Z_{\perp}$.

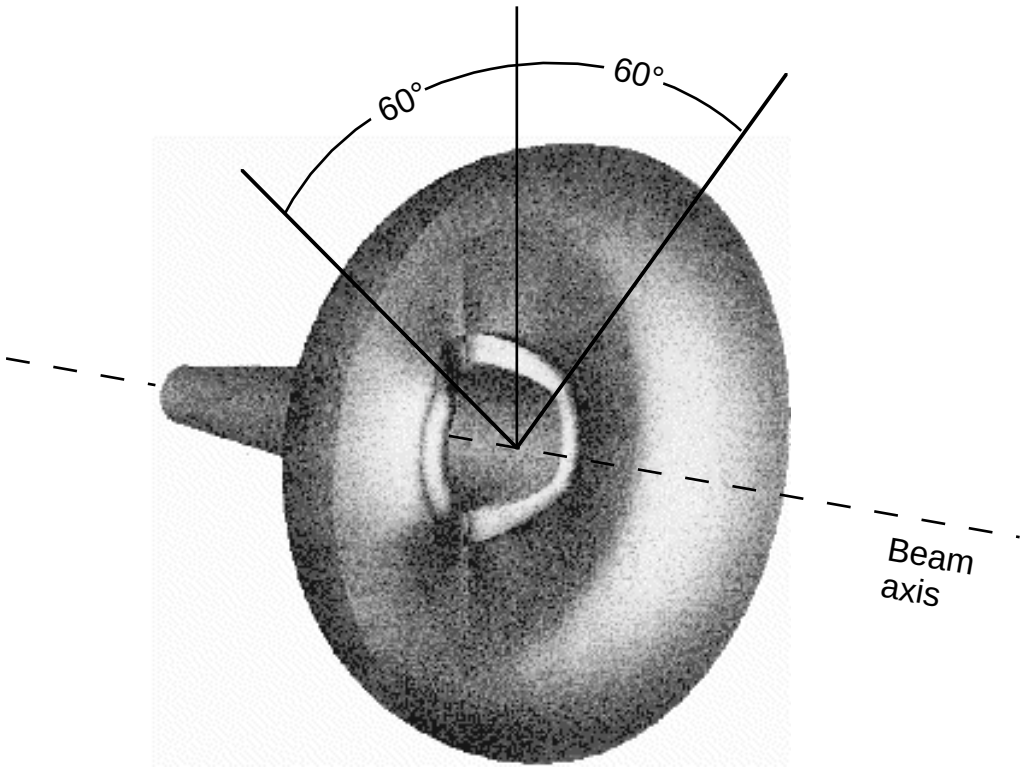

Figure 5: Internal view of the nose-cone cavity, showing the deformation of the nose needed to remove the degeneracy of the deflecting modes.

Table 3

Mode type	Res. freq. [MHz]	Re{Z_p} [kΩ]	Re{Z_{Ph}} [kΩ/mm]	Re{Z_{Pv}} [kΩ/mm]	Q-factor
monopole	231.63	4837	==	==	41341
hor. dipole	363.30	==	27.10	==	40907
vert. dipole	410.15	==	==	13.50	48802
hor. dipole	443.78	==	1.950	==	33387
vert. dipole	457.69	==	==	0.221	49222
monopole	465.84	262.0	==	==	38500

The next step in the cavity design is dimensioning the waveguide dampers. We chose reduced-height rectangular waveguides (370 mm × 50 mm), which have a cut-off frequency of 405 MHz, just below the resonant frequency of the first vertical dipole mode (410.15 MHz). We performed many simulations to investigate how the orientation of the waveguides and their location on the cavity influence the HOM damping.

The best results were achieved with waveguides running parallel to the beam axis, at a distance of 200 mm from it (this is the minimum distance that keeps the waveguide openings outside the nose region). Table 4 shows the parameters of interest for the cavity with waveguides terminated by matched loads, characterised up to 1000 MHz. Dampers are quite effective to lower the coupling impedance values and the Q-factors of the HOMs, included the first vertical dipole mode. Only a few modes have still a Q-factor of the order of thousands, but their impedance values are quite small. The effect on the first horizontal dipole mode is mainly a slight decrease of its resonant frequency, due to the modification of the geometry introduced by the insertion of the waveguides. Of course, the first monopole mode is practically undamped, since its resonant frequency is far below the cut-off frequency of the waveguide dampers. The instability rise times of the HOMs have values high enough to be damped with the bunch-by-bunch feedback system [12], while the fundamental mode has to be treated separately.

Table 4

Mode type	Res. freq. [MHz]	Re{$Z_{\parallel}$} [kΩ]	Re{$Z_{\perp h}$} [kΩ/mm]	Re{$Z_{\perp v}$} [kΩ/mm]	Q-factor
monopole	225.77	4057	==	==	57808
hor. dipole	360.75	==	26.27	==	44380
monopole	407.64	0.700	==	==	2505.0
vert. dipole	410.97	==	==	0.106	435.00
hor. dipole	469.83	==	0.002	==	27.000
hor. dipole	510.08	==	0.087	==	1340.0
hor. dipole	588.14	==	0.003	==	4561.0
vert. dipole	623.74	==	==	0.039	664.00
hor. dipole	654.27	==	0.020	==	3576.0
vert. dipole	670.90	==	==	0.007	1087.0
hor. dipole	754.23	==	0.006	==	533.00
monopole	765.88	0.220	==	==	42.000
hor. dipole	854.80	==	0.002	==	169.00
monopole	876.53	1.200	==	==	32426
vert. dipole	884.61	==	==	0.009	500.00
vert. dipole	939.75	==	==	0.007	623.00

6.2 Rounded Cavity

Also for the rounded cavity, the first design step is the modification of the geometry in figure 2, necessary to remove the dipole mode degeneracy. In this case we considered an elliptical cross-section of the cavity in correspondence of the γ plane (see figure 4b), with the major axis in the horizontal plane. Numerical simulations were performed to dimension the two axes of the ellipse in order to have the correct splitting of the resonant frequencies for the first horizontal and vertical dipole modes.

Figure 6 shows the geometry of the resulting modified rounded cavity (without dampers).

The monopole and dipole modes of the cavity are characterised up to 550 MHz in table 5.

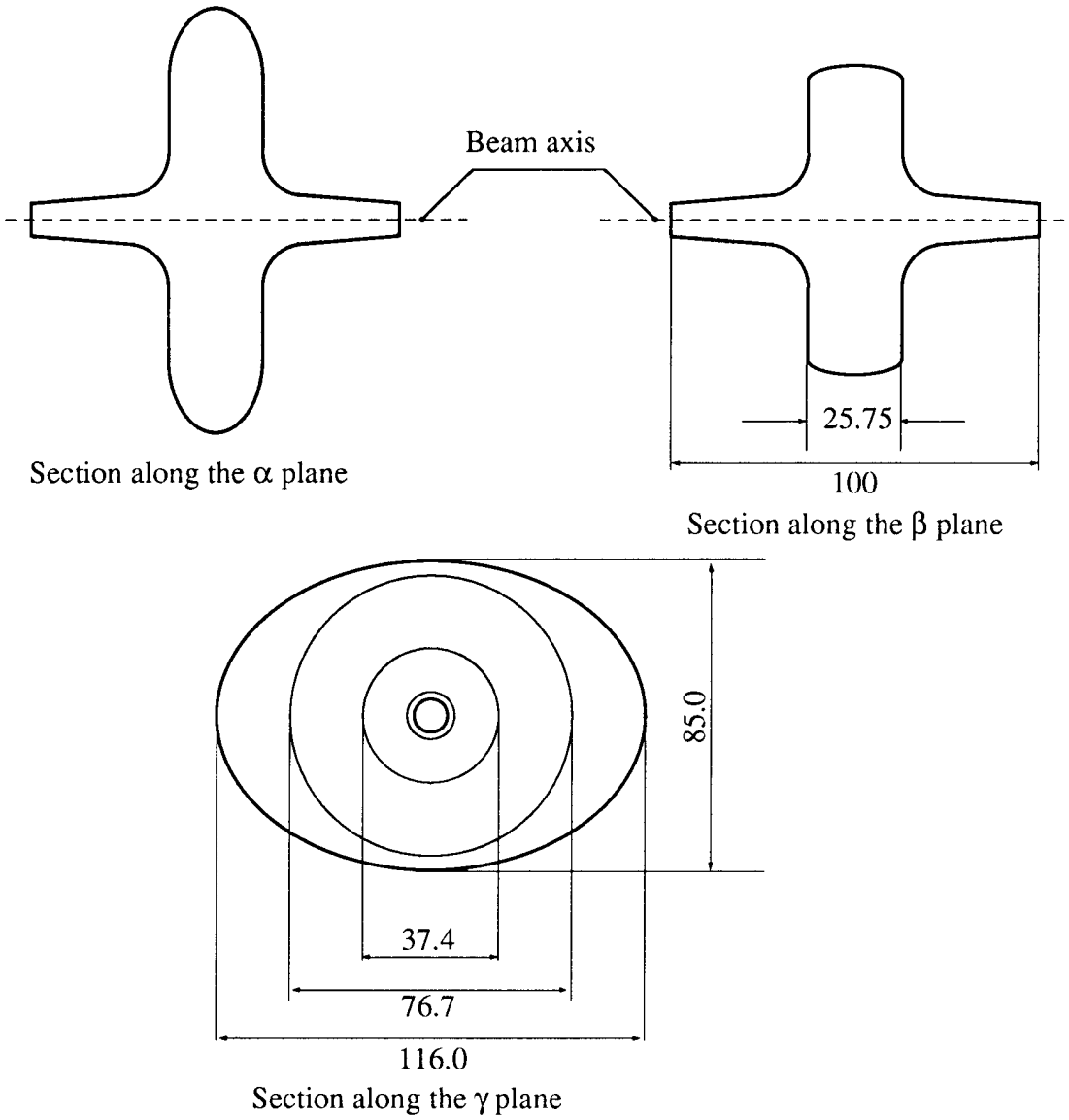

Figure 6: Geometry of the modified rounded cavity (without waveguide dampers). The labelling of the planes is the same as in Figure 4. All dimensions in cm.

Table 5

Mode type	Res. freq. [MHz]	Re{$Z_{\parallel}$} [kΩ]	Re{$Z_{\perp h}$} [kΩ/mm]	Re{$Z_{\perp v}$} [kΩ/mm]	Q-factor
monopole	268.99	3230	==	==	42177
hor. dipole	361.15	==	14.50	==	51356
vert. dipole	409.51	==	==	15.90	52729
monopole	536.44	222.0	==	==	60000

Then simulations have been performed to find the most effective orientation and location of the waveguides for the HOMs damping. We found that reduced-height rectangular waveguides of 375 mm × 80 mm (cut-off frequency = 400 MHz), with axes running parallel to the beam axis at a distance of 240 mm give the best performance. Note that the large lateral walls of the rounded cavity allow the use of waveguides that are a little bit larger than those used in the nosecone cavity design, a feature that makes HOMs damping easier.

Table 6 shows, up to 1000 MHz, the parameters of interest for the monopole and dipole modes of the rounded cavity with waveguides terminated by matched loads. Dampers are very effective to decrease the coupling impedance values and the Q-factors of the HOMs, included the first vertical dipole mode. In fact, apart from the first monopole and the mode used for the crabbing operation, no modes survive with Q-factors larger than 700, and the coupling impedances are all very low, giving rise times of the order of msec in the 30 bunch operation mode of DAΦNE. Also for the rounded cavity, the fundamental mode has to be treated separately.

Table 6

Mode type	Res. freq. [MHz]	Re{$Z_{\parallel}$} [kΩ]	Re{$Z_{\perp h}$} [kΩ/mm]	Re{$Z_{\perp v}$} [kΩ/mm]	Q-factor
monopole	245.18	2835	==	==	34333
hor. dipole	363.05	==	13.88	==	49528
vert. dipole	406.62	==	==	0.039	98.000
vert. dipole	567.25	==	==	0.003	43.000
monopole	606.92	0.473	==	==	52.000
vert. dipole	679.56	==	==	0.005	42.000
hor. dipole	685.43	==	0.009	==	229.00
monopole	710.17	0.23	==	==	530.00
hor. dipole	754.78	==	0.008	==	666.00
monopole	879.01	0.832	==	==	143.00
monopole	883.57	0.473	==	==	218.00
hor. dipole	908.65	==	0.004	==	159.00
vert. dipole	949.63	==	==	0.011	248.00
hor. dipole	972.37	==	0.009	==	115.00
vert. dipole	986.32	==	==	0.005	86.000

7. Conclusions

A comparison between the two geometries shows that the nosecone cavity is better performing as far as the coupling impedance of the horizontal dipole mode is concerned: in fact, its value is about twice that obtained from the rounded cavity. The HOMs damping in the nosecone cavity, however, is poorer than in the rounded one, since in the former some modes survive with rather high Q-values, even in presence of the waveguide dampers. This is due to the concentration of the HOMs fields in the axial region produced by the nose, a fact that reduces the coupling with the waveguides and thus their effectiveness in removing the energy associated to the HOMs. On the contrary, in the rounded cavity the energy associated to the HOMs is more evenly distributed, thus making its removal through the waveguides easier. As a result, the rounded crab cavity has only one parasitic mode, i.e., the first monopole, all other parasitic modes exhibiting very low Q-factors and coupling impedances.

From the point view of instabilities, despite the higher shunt impedances of HOMs of the nosecone cavity, there is no substantial difference and both cavities could in principle be used, the residual multibunch instability being controlled by a bunch- by- bunch feedback system. However the rounded cavity is easier to manufacture because of its less complex shape, and its drawback of having a relatively lower impedance at the mode of operation can be easily overcome by operating it with a larger input power.

References

[1] Proposal for a Φ-Factory, p. 365, LNF - 90 /031 (R) (1990).
[2] Beijing Tau- Charm Factory, IHEP- BTCF Report- 03, October 1996.
[3] T. Chen, D. Rice, D. Rubin, D. Sagan. M. Tigner, "Experimental Study of Crossing Angle Collision", SLAC - PUB - 6214, May 1993. Presented at 1993 Particle Accelerator Conference (PAC 93), Washington, DC, 17- 20 May 1993.
[4] D.L. Rubin, M. Billing, J. Byrd, T. Chen, Z. Greenwald, D. Hartill, J. Hylas, J. Kaplan, A. Krasnykh, R. Meller, S. Peck, T. Pelaia, D. Rice, D. Sagan, L.A. Schick, J. Sikora, J. Welch, "Beam- Beam Interaction with a Horizontal Crossing Angle", Nucl. Inst. and Meth. A330: 12-20, 1993.
[5] K. Cornelis, W. Herr, A. Piwinski, "Experimental Study of Electron Positron Collisions in LEP with a Finite Crossing Angle", European Particle Accelerator Conference, Berlin, Germany, March 24- 28, 1992.
[6] M. Zobov, K. Hirata, "Beam- Beam Interaction Study for DAΦNE", Fifth European Particle Accelerator Conference (EPAC 1996), Sitges, Barcellona, 10- 14 June 1996.
[7] R. Palmer, SLAC - PUB - 4707 (1988).
[8] KEKB B-Factory Design Report 95-7, June, 1995.
[9] G. P. Jackson, Workshop on beam dynamics issue of "High Luminosity Asymmetric Colliders Rings", Berkeley (1990).
[10] K. Oide and K. Yokoya, "The Crab Crossing Scheme for Storage Ring Colliders", Phys. Rev. D 40,315 (1989).
[11] R. Boni, F. Caspers, A. Gallo, G. Gemme, R. Parodi, "A Broadband Waveguide to Coaxial Transition for High Order Mode Damping in Particle Accelerator RF Cavities", Particle Accerators, Vol. 45, (1994) p. 195.
[12] S. Bartalucci, M. Bassetti, R. Boni, S. De Santis, A. Drago, A. Gallo, A. Ghigo, M. Migliorati, L. Palumbo, R. Parodi, M. Serio, B. Spataro, G. Vignola, and M. Zobov, "Analysis of Methods for Controlling Multibunches Instabilities in DAΦNE", Particle Accelerators, 1995, Vol. 48, pp. 213 - 217.
[13] M. Zobov, et al., "Collective Effects and Impedance Study for DAΦNE Φ-Factory", LNF-95/041 (P), 1995.
[14] S. Bartalucci, B. Spataro, "A Crabbing Cavity for DAΦNE", Note RF - 10, Frascati 1993.
[15] T. Weiland, "On the computation of Resonant Modes in Cylindrically Symmetric Cavities", Nuclear Instruments and Methods, NIM 216 (1983) p. 329-348.
[16] P. Arcioni, G. Conciauro: "Feasibility of HOM-Free Accelerating Resonators: Basic Ideas and Impedance Calculations", Particle Accelerators, Vol. 36, pp. 177 203, 1991.
[17] P. Arcioni, M. Bressan, L. Perregrini: "A New Boundary Integral Approach to the Determination of Resonant Modes of Arbitrarily Shaped Cavities", IEEE Trans. on Microwave Theory and Techniques, MTT-43 no. 8, pp. 1848-1856, Aug. 1995.
[18] S. Bartalucci, L. Palumbo, M. Serio, B. Spataro, M. Zobov, "Broad - Band Model Impedance for DAΦNE Main rings", Nucl. Inst. Meth. A 337, 1994, pp. 231 - 241.
[19] W. P. Kilpatrick, "Criterion for Vacuum Sparking Designed to include both RF and DC", VCRL - 2331-Sept. 1953.
[20] D. Boussard, H. P. Kindermann and V. Rossi, " RF feedback applied to a multicell superconducting cavity", Proc. of the 1st European Particle Accelerator Conference (EPAC), Rome 1988, p. 985.